

STUDIES ON THE NON-ISOTHERMAL DECOMPOSITION OF $H_3PMO_{12}O_{40} \cdot xH_2O$ AND $H_4PVMO_{11}O_{40} \cdot yH_2O$

V. Sasca¹, M. Ștefănescu² and A. Popa¹

¹Romanian Academy – Timișoara Branch, Bd. M. Viteazul 24, RO-1900 Timișoara

²Faculty of Industrial Chemistry and Environmental Engineering, The Polytechnical University, RO-1900 Timișoara, Piata Victoriei nr. 2, Romania

Abstract

This paper reports a comparative study of the non-isothermal decompositions of the heteropolyacids HPM and HPVM, with structures consisting of Keggin units (KUs). Non-isothermal analysis at low heating rates demonstrated the existence of 4 crystal hydrate species, depending on the temperature. The stability domains of the anhydrous forms of HPM and HPVM were found to be 150–380°C, respectively. Processing of the TG curves obtained at different heating rates by the Ozawa method revealed that the decomposition of anhydrous HPM takes place according to a unitary mechanism, whilst for anhydrous HPVM two mechanisms are observed. Thus, the first part of the constitution water is lost simultaneously with the departure of vanadium from the KU as VO^{2+} , while the second part is lost at higher temperatures as in the case HPM.

Keywords: heteropolyacids, isoconversional method, non-isothermal analysis

Introduction

The heteropolyacids with Keggin structure behave as bifunctional catalysts since they possess both an acid function due to the Brönsted acidity and a redox function due to the oxygen transfer capacity [1–9]. Most frequently used are molybdophosphoric acid, $H_3PMO_{12}O_{40}$ (HPM), and 1-vanado-11-molybdophosphoric acid, $H_4PVMO_{11}O_{40}$ (HPVM), in consequence of their appropriate catalytic activity in the selective oxidation of unsaturated aldehydes [1], the oxydehydrogenation of isobutyric acid [7, 8] and the oxidation of lower alcohols [10].

Deactivation of these catalysts may occur due to the relatively low thermal stability, which may result in their decomposition under certain reaction conditions [1, 5, 6, 10]. The thermal stabilities of these compounds can be studied by various methods, e.g. thermogravimetric analysis [1, 3, 5, 7, 8, 10]; differential thermal analysis [2, 4, 7]; IR (KBr pellet) [4, 5, 7, 8, 10] and 'in situ' spectroscopy [5, 10]; NMR [1, 6, 7, 9]; powder, monocrystal [2, 4, 7, 9] and 'in situ' [9] diffraction analysis; transmission, analytical [1] and scanning [1, 10] electronic microscopy and ESR [1, 9].

The most commonly used method is thermogravimetric analysis, since the Keggin structure may be destroyed by the elimination of water molecules formed from

the corresponding mass loss as functions of temperature and the working atmosphere. This allows for a relatively easy determination of the kinetic parameters.

The present paper provides new data concerning the mechanism and kinetics of the decompositions of the above acids, resulting from analysis of the thermal decomposition curves obtained by the methods of non-isothermal kinetics.

Experimental

Sample preparation

HPM was prepared by adding p.a. MoO_3 to a boiling aqueous solution of p.a. H_3PO_4 in stoichiometric ratio, followed by continued boiling for 2–3 h, filtration of the solution, extraction of HPM with diethyl ether as an oily adduct heavier than water, decomposition of the adduct by water addition, elimination of the ether by air bubbling, and separation of HPM by crystallization from the aqueous solution.

HPVM was prepared by the method of Tsigdinos and Hallada [11]. Samples of HPM and HPVM were heated at 270, 300 and 330°C for 4 h.

Thermogravimetric analysis

This was carried out with a derivatograph analyser system (Paulik, Paulik, Erdey type D, (MOM, Budapest)), with ceramic and platinum crucibles, a sample mass of 100–800 mg, at heating rates of 1.25–10°C min^{-1} under static air atmosphere. HPM samples of 100 mg were deposited on an inert support (quartz; $\phi=0.1\text{--}0.2$ mm).

Characterization of the samples

This was carried out by pH titration in aqueous solution with a 0.1 M NaOH solution with a glass-electrode pH-meter MV-84 (Carl Zeiss, Jena) in the pH range 2–11.

The UV-VIS spectra of the two acids were recorded with a Specord M42 instrument (Carl Zeiss, Jena) between 240 and 520 nm.

The IR spectra of HPM and HPVM in KBr pellets were recorded with a Specord M 80 instrument (Carl Zeiss, Jena) between 200 and 2000 cm^{-1} , and a Shimadzu IR 460 instrument between 400 and 2000 cm^{-1} .

Diffraction analysis investigations were carried out on powders of the acids with a TUR 61 instrument.

Results and discussion

The processes taking place during the thermal decompositions of HPM and HPVM affect the existence of the primary and secondary structures [12–14]. The primary structure of the Keggin anion ($\text{XM}_{12}\text{O}_{40}^{X-}$) also named the Keggin unit (KU), is presented in Fig. 1, where $X=\text{P}$, As or Si , and $M=\text{Mo}$, W , or V . A central tetrahedron (XO_4) determining the molecular symmetry is surrounded by four octahedral

groups (M_3O_{12}), each consisting of three octahedra with M in the centre (MO_6) with two common edges. The four octahedral groups are bonded through vertices.

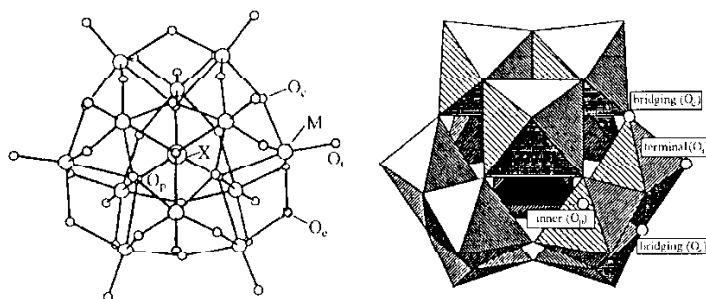


Fig. 1 Keggin unit structure ($XM_{12}O_{40}^{3-}$): a – larger circles, central and peripheral atoms; smaller circles, oxygen atoms; b – the central tetrahedron XO_4 (darkened) and the surrounding M_3O_{12} octahedral groups [15]

HPM consists of KU with normal structure (spherical form), whilst HPVM consists of KU with reversed structure (more prolonged on an axis) due to the replacement of one Mu^{6+} for a V^{5+} , resulting in an electron deficiency in the polyanion and a rearrangement of the primary structure.

The anions are interconnected by bridges of 2 or even 3–4 water molecules, to which the protons are hydrogen-bonded (Fig. 2). This results in an arrangement with large, communicating spaces, forming a tridimensional network of channels in which water molecules are randomly situated. The resulting structure is known as the secondary structure and involves the relative orientations of the anions, and the arrangements of the crystallization water and the protons in a semirigid network.

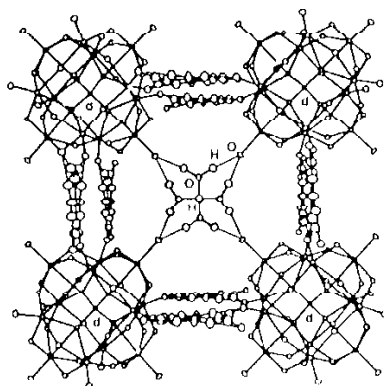


Fig. 2 Structural arrangement of anions, protons and water molecules in 12-tungstophosphoric acid [16]

The packing of the normal KUs is closer and the arrangement of the water molecules between the units is more ordered. Consequently, the diffraction spectra of HPM and HPVM indicate different structures, depending on the hydration degree. With decrease of the hydration degree, the spectra of the two acids become ever closer [9].

The usual methods for the preparation of HPM and HPVM afford crystal hydrates with a variable number (13–32) of water molecules [1, 3, 5, 6, 8, 9]. Highly hydrated species generally result, with 29–32 water molecules, which are subsequently transformed into room-temperature stable crystal hydrates containing 13–14 molecules of water [5, 8]. The experimental results confirm the literature data: the synthesis furnishes acids with a high hydration degree, which gradually falls when the products are kept at room temperature and stabilizes at $14 \pm 1.5\text{H}_2\text{O}$ depending on the temperature and the atmospheric humidity.

The diffraction spectra of the crystal hydrates with 13–14 H_2O molecules presented in Fig. 3 have the main diffraction maxima at close angles (differences less than 1°), the intensities of the maxima being higher for HPVM, due to the formation of larger crystals. The diffraction spectra of HPM and HPVM calcined at 300°C are significantly different, which means that modifications have occurred in the structure of HPVM, because thermal analysis demonstrates that HPM is stable at 300°C , and the structures of the two acids should be approximately identical after the elimination of the hydration water, which takes place at temperatures up to 200°C .

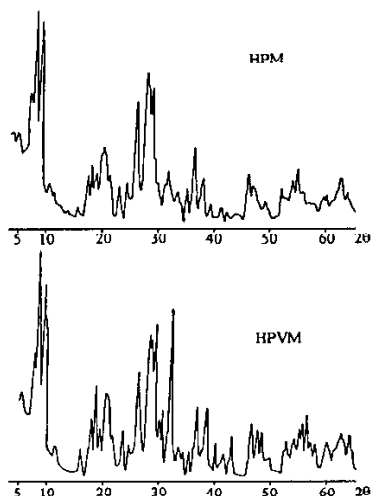


Fig. 3 Powder diffraction patterns (Cu radiation) of HPM and HPVM-13–14 H_2O

Analysis of the thermal curves obtained under non-isothermal conditions reveals the following principal decomposition processes: elimination of the hydration water in several steps, decomposition of the anhydrous acids with elimination of the con-

stitutive water (all accompanied by endothermic effects), and the process of crystallization of MoO_3 , accompanied by an exotherm.

The most informative and reproducible results were obtained with 300 mg samples in platinum crucibles; thermal curves thus obtained are presented in Fig. 3. Previous studies indicated that the hydration water (consisting of residual water, adsorbed water and crystallization water) is lost in several steps. This has led to the claim [9] of the existence of intermediate crystal hydrates with 24 water molecules, 14 (triclinic structure) water molecules, and 6 water molecules, the last of these obtained directly from the species containing 24 water molecules without formation of the intermediate hydrate by heating at 57°C . In an other study [7], the hydration water is lost between 120 and 180°C for HPVM, with DTG maxima at 105, 135 and 160°C , or both HPM and HPVM containing 13 water molecules are converted at $60\text{--}80^\circ\text{C}$ to an unstable intermediate (probably cubic) containing 7–8 water molecules, which is subsequently transformed at $100\text{--}350^\circ\text{C}$ to the anhydrous (tetragonal) species. From Fig. 4 for HPM and HPVM DTG maxima may be observed at 40, 57, 87 and 102°C , and at 42, 58, 90 and 102°C , respectively, accompanied by endothermic effects.

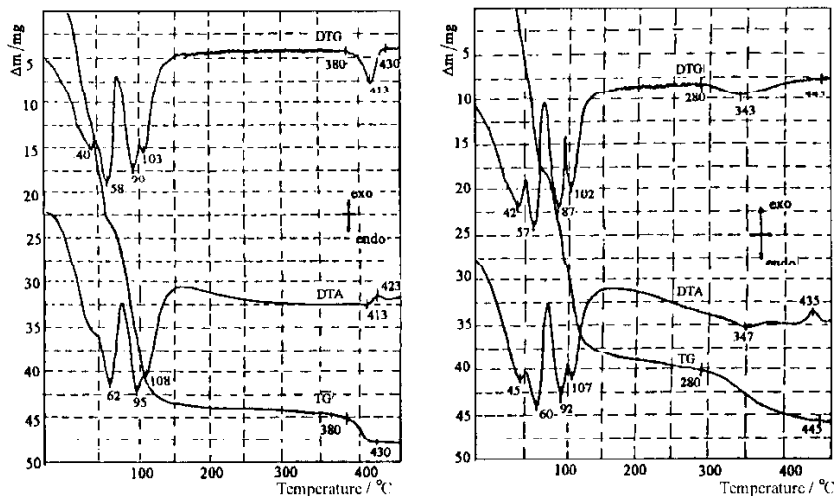


Fig. 4 Thermoanalytical curves of samples of a – HPM and b – HPVM (sample mass=300 mg, heating rate= $2.5^\circ\text{C min}^{-1}$, Pt plates crucible, static air atmosphere)

The DTG and DTA peaks may be assigned to bonded water from the crystal hydrates with 20–24, 12–14, 8–9 and 3–4 water molecules. The residual water is lost in a diffuse way without a DTG maximum or a detectable thermal effect. The process of hydration water elimination ends at a temperature of about $150\text{--}200^\circ\text{C}$, depending on the working conditions. It is to be mentioned that for HPVM another slight mass loss is observed, at higher temperatures.

It may be considered that, between 150 and 280°C for HPVM and between 150 and 380°C for HPM, both acids are stable as anhydrous species; subsequently, they decompose with the loss of constitutive water and the transformation of HPM into MoO_3 and P_2O_5 , and of HPVM into MoO_3 , P_2O_5 and V_2O_5 .

The final process evidenced is the crystallization of MoO_3 . The temperature ranges for these processes depend on the working conditions; generally, with lower heating rates they shift towards lower temperature; this is more obvious at the temperatures corresponding to the peaks in the DTG and DTA curves.

The literature data indicate that vanadium leaves the network of KU as VO^{2+} . It is presumed that VO^{2+} is a stabilizer for the Keggin structure because it replaces some of the protons and binds the KU together [5, 6, 8]. An NMR study of HPVM subjected to thermal treatment revealed that vanadium leaves the KU together with the constitutive water, and at 320°C only 49% of the vanadium remains in the KU after some hours. An anhydrous species was identified in low amount, $\text{H}_5\text{PV}_2\text{Mo}_{10}\text{O}_{40}$ (HPV₂M), together with the anhydrous species of HPVM; thus, it may be concluded that solid-state reactions took place. It follows that the elimination of the constitutive water from the anhydrous species of HPVM takes place in the first stage by the replacement of the protons by VO^{2+} . This explains the lower temperature at which the process starts with respect to HPM (280–290°C, as compared to 380–400°C, depending on the experimental conditions). The subsequent decomposition of the KU is similar to that of the KU of the acid HPM.

The upper temperature limit for the decomposition range is higher for HPVM, because of the stabilizing effect of VO^{2+} on the Keggin structure (440–465°C, as compared to 420–450°C for HPM).

According to the isoconversional methods of Ozawa and Flynn-Wall, a plot of $\log \alpha$ as a function of $1/T$, for $\alpha = \text{constant}$, will give parallel straight lines if the mechanism of the decomposition is the same within the range of studied conversion degrees. Such plots for four heating rates (1.25, 2.5, 5 and 10 deg min^{-1}) gave straight lines with a low dispersion of the points, and thus the slopes have reliable values, only for a sample mass of 100 mg, and (in the case of HPM) only as a coating deposited on an inert support. Nevertheless, at a heating rate of 10 deg min^{-1} , the points exhibited a significant deviation from linearity, and these points were therefore excluded from the calculations.

The slopes of the straight lines depicted in Figs 5 and 6 suggest the existence of a uniform mechanism of decomposition in the range of α from 0.1 to 0.8 for HPM, and two mechanisms in the case of HPVM. The first mechanism holds for α values from 0.1 to 0.4, and the second for α values from 0.5 to 0.8.

The activation energies calculated by the Ozawa-Flynn-Wall methods are given in Tables 1 and 2. The activation energies were calculated for separate TG curves corresponding to various heating rates for the integral form ($F(\alpha)$) of the relationship [17]:

$$f(1 - \alpha) = (1 - \alpha)^n \quad (1)$$

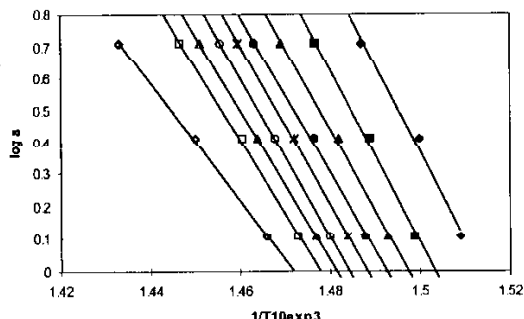


Fig. 5 Isoconversional plots for the thermal decomposition of HPM at various heating rates (1.25, 2.5 and 5°C min⁻¹)

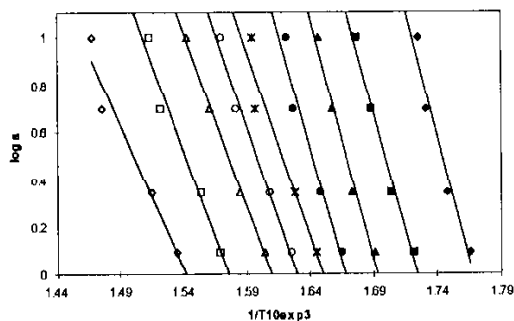


Fig. 6 Isoconversional plots for the thermal decomposition of IIPVM at various heating rates (1.25, 2.5 and 10°C min⁻¹)

The best fits to the experimental points were obtained for $n=1.9$. An average activation energy of 155 ± 5 kJ mol⁻¹ was found for HPVM (α variation from 0 to 1) in comparison with an average value of 150.5 ± 6.6 kJ mol⁻¹ ($\alpha=0.1-0.4$) and of 114.3 ± 4.7 kJ mol⁻¹ ($\alpha=0.5-0.8$) (Table 1). For IIPM, an average value of 737.4 ± 40 kJ mol⁻¹ (α variation from 0 to 1) was found, in comparison with an average value of 188.8 ± 17.8 kJ mol⁻¹ ($\alpha=0.1-0.8$) (Table 2). A good agreement was obtained between the average activation energies for the two calculation methods in the case of HPVM within the range of α from 0.1 to 0.4 only; consequently, the $(F\alpha)$ used is not an appropriate relationship in other situations.

The elimination of the constitution water is considered to proceed through VO²⁺ taking over the binding role of H₃O⁺ and H₅O₂⁺. The changes in the IR spectra of HPM and HPVM as a function of temperature furnish valuable information on the process of release of vanadium from the host structure. For the interpretation of the IR spectra of HPM and HPVM, the range of frequencies 1100–900 cm⁻¹ was selected (Fig. 7), where characteristic absorption bands occur: the band at 1064 cm⁻¹

Table 1 Kinetic data and evaluation of the activation energy according to Ozawa and Flynn-Wall for HPVM

Degree of conversion α	Temperature T , K for various heating rates $a/^\circ\text{C min}^{-1}$				Activation energy/ kJ mol^{-1}
	1.25	2.5	5	10	
0.1	566.2	572.1	577.7	579.0	157.1
0.2	580.7	586.8	592.8	596.6	148.3
0.3	591.4	597.7	603.5	607.5	152.1
0.4	600.6	606.8	615.0	616.9	144.6
0.5	607.9	614.2	626.2	627.3	117.7
0.6	615.4	621.8	632.5	636.9	119.0
0.7	623.3	630.1	640.6	648.0	109.8
0.8	636.9	643.5	657.0	660.9	110.6
0.9	651.5	659.6	677.5	681.2	92.2

Average value for $\alpha=0.1-0.4 = 150.5 \pm 6.5 \text{ kJ mol}^{-1}$; for $\alpha=0.5-0.8 = 114.3 \pm 4.7 \text{ kJ mol}^{-1}$

Table 2 Kinetic data and evaluation of the activation energy according to Ozawa and Flynn-Wall for HPM

Degree of conversion α	Temperature T , K for various heating rates $a/^\circ\text{C min}^{-1}$			Activation energy/ kJ mol^{-1}
	1.25	2.5	5	
0.1	662.7	666.7	672.5	206.6
0.2	667.1	671.6	677.0	203.6
0.3	669.7	674.8	680.7	191.1
0.4	672.0	677.0	683.5	183.5
0.5	673.8	679.3	684.9	187.7
0.6	675.7	681.2	686.8	187.7
0.7	677.0	683.0	689.1	176.8
0.8	678.9	684.5	691.1	173.5
0.9	682.1	689.6	697.8	139.5

Average value for $\alpha=0.1-0.8 = 188.8 \pm 17.8 \text{ kJ mol}^{-1}$

was assigned to the vibration $\nu_{\text{as}}(\text{P}-\text{O}_{\text{p}})$, and that at 964 cm^{-1} to the vibration $\nu_{\text{as}}(\text{M}-\text{O})$, while the shoulders at 1080 and 1000 cm^{-1} were characteristic of the V^{5+} included in the KII structure. The gradual disappearance of these shoulders with increasing temperature from 270 to 330°C proves the existence of a correlation between the constitution water elimination and the vanadium release from the KU structure for HPVM.

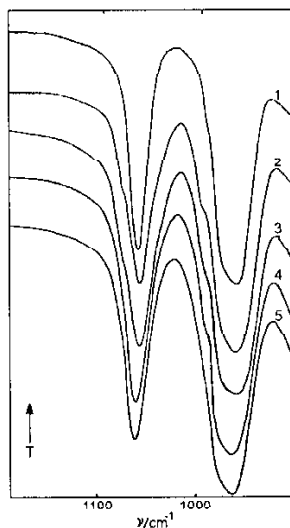


Fig. 7 IR spectra of HPM (1) and HPV (2–5): 1, 2 – fresh samples; 3 – after thermal treatment at 270°C for 4 h; 4 – at 300°C for 4 h; 5 – at 330°C for 4 h

Conclusions

Evidence has been found for four species of crystal hydrates that are specific for both acids: 20–24, 12–14, 8–9 and 3–4H₂O.

A rapid variation of the hydration degree has been observed for both acids with respect to temperature and atmospheric humidity.

The thermal stability ranges for the two acids are different: 150–280°C for HPV, and 150–380°C for HPM. The upper temperature limit for the presence of KU in the lattice of the acid is 15–20°C higher for HPV.

The explanation proposed for the decrease of the lower limit, and the increase in the upper limit for the temperature range relating to the decomposition of HPV is that vanadium leaves the KU as VO²⁺. This results in the elimination of H⁺ as H₂O at lower temperatures and bonding for the KU through VO²⁺, the stability of the lattice being increased in this way.

Kinetic analysis of the TG curves by isoconversional methods demonstrates the existence of two mechanisms for the thermal decomposition of HPV, but the average activation energies calculated are not in good agreement with the average activation energies calculated with the $F(\alpha)$ form (1) for the individual TG curves at various heating rates.

This final conclusion will be returned to and investigated in a future paper by means of IR spectroscopy and X-ray diffractometry, and other forms of the function $F(\alpha)$ will be tested.

References

- 1 J. B. Black, N. J. Clayden, P. L. Gai, J. D. Scott, E. M. Serwiecka and J. R. Goodenough, *J. Catal.*, 106 (1987) 1.
- 2 G. B. McGarvey and J. B. Moffat, *Catal. Lett.*, 16 (1992) 173.
- 3 L. C. Josefowicz, H. G. Karge, E. Vasilyeva and J. B. Moffat, *Micr. Mat.*, 1 (1993) 313.
- 4 G. B. McGarvey, N. J. Taylor and J. B. Moffat, *J. Mol. Catal.*, 80 (1993) 59.
- 5 C. Rocchiccioli-Deltcheff and M. Fournier, *J. Chem. Soc. Faraday Trans.*, 87 (1991) 3913.
- 6 B. Taouk, D. Ghoussoub, A. Bennani, E. Crusson, M. Rigole, A. Aboukais, R. Decressain, M. Fournier and M. Guelton, *J. Chim. Phys.*, 89 (1992) 435.
- 7 C. Marchal, A. Davidson, R. Thouvenot and G. Herve, *J. Chem. Soc. Faraday Trans.*, 89 (1993) 3301.
- 8 E. Cadot, C. Marshal, M. Fournier, A. Teze and G. Herve, in *Polyoxometalates*, M. T. Pope and A. Muller (eds), Kluwer Dordrecht, 1994, p. 315.
- 9 B. Herzog, W. Bensch, Th. Ilkenhans and R. Schlogl, *Catal. Lett.*, 20 (1993) 203.
- 10 K. Bruckman, M. Che, J. Haber and J. M. Tatibouet, *Catal. Lett.*, 25 (1994) 225.
- 11 G. A. Tsigdinos and C. J. Hallada, *Inorg. Chem.*, 7 (1968) 437.
- 12 H. d'Amour and R. Allmann, *Z. Kristallogr.*, 143 (1976) 1.
- 13 V. A. Sergienko, M. A. Porai-Koshits and E. N. Yurchenko, *J. Struct. Chem.*, 21 (1980) 87.
- 14 H. T. Evans and M. T. Pope, *Inorg. Chem.*, 23 (1984) 501.
- 15 J. F. Keggin, *Nature (London)*, 131 (1933) 908; *Proc. R. Soc. London Ser. A* 144 (1934) 75.
- 16 G. M. Brown, M. R. Noc-Spirlet, W. R. Busing and H. A. Levy, *Acta Cryst. Sect. B* 33 (1977) 1038.
- 17 C. Popescu, E. Segal and C. Oprea, *J. Thermal Anal.*, 38 (1992) 929.